

Supporting information for

A Novel π -d Conjugated Cobalt Tetraaza[14]annulene based Atomically Dispersed Electrocatalyst for Efficient CO₂ Reduction

Zhifu Liang^{1,3 +}, Ting Zhang^{1,3 +}, Pengfei Cao^{2,7 *}, Takefumi Yoshida⁴, Weiqiang Tang^{5*}, Xiang Wang³, Yong Zuo³, Pengyi Tang⁶, Marc Heggen⁷, Rafal E. Dunin-Borkowski⁷, Joan Ramon Morante³, Andreu Cabot^{3*}, Masahiro Yamashita^{8,9}, Jordi Arbiol^{1,10 *}

Z. F. Liang, Dr. T. Zhang, Prof. J. Arbiol

¹Catalan Institute of Nanoscience and Nanotechnology (ICN2), CSIC and BIST

Campus UAB, Bellaterra, 08193 Barcelona, Catalonia, Spain

Dr. P. F Cao

²School of Chemical Engineering and Technology, Xi'an Jiaotong University, Xi'an 710049, China

Z. F. Liang, Dr. T. Zhang, X. Wang, Y. Zuo, Prof. J. R. Morante, Prof. A. Cabot

³Catalonia Institute for Energy Research - IREC

Sant Adrià de Besòs, Barcelona, 08930, Catalonia, Spain

Dr. Takefumi Yoshida

⁴Innovation Research Center for Fuel Cells,

The University of Electro-Communications, Chofu, Tokyo 182-8585, Japan

Dr. W. Tang

⁵State Key Laboratory of Chemical Engineering and School of Chemical Engineering, East China University of Science and Technology, Shanghai, 200237, China

Prof. P. Y. Tang

⁶ShangHai Institute of Microsystem and Information Technology, Chinese Academy of Sciences, Shanghai 200050, China

Dr. P. F Cao, Dr. P. Y Tang, Dr. M Heggen, Prof. R E. Dunin-Borkowski

⁷Ernst Ruska-Centre for Microscopy and Spectroscopy with Electrons and Peter Grünberg Institute Forschungszentrum Jülich GmbH 52425 Jülich, Germany

Prof. Masahiro Yamashita^{8,9}

⁸Department of Chemistry, Graduate School of Science, Tohoku University

6-3 Aramaki-Aza-Aoba, Aoba-Ku, Sendai 980-8578, Japan

⁹School of Materials Science and Engineering, Nankai University, Tianjin 300350, China

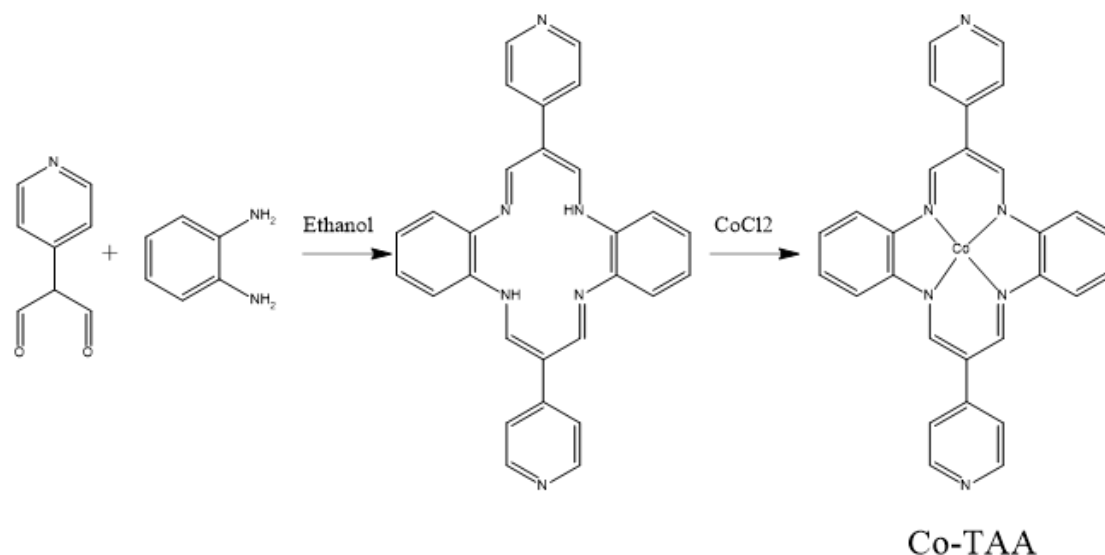
Prof. A. Cabot, Prof. J. Arbiol

¹⁰ICREA

Pg. Lluís Companys 23, 08010 Barcelona, Catalonia, Spain

⁺ These authors Zhifu Liang and Ting Zhang contribute equally to this work

*Corresponding author. E-mail: p.cao@fz-juelich.de, wqtang@ecust.edu.cn, acabot@irec.cat, arbiol@icrea.cat



Scheme S1. Scheme of the synthesis of Co-TAA

The control sample Co-TAA was prepared following procedures found in the literature.^[S1]

2-(4-Pyridyl)malondialdehyde (149 mg, 1 mmol), o-Phenylenediamine (108 mg, 1 mmol) and 8 mL Ethanol were added to a 25 mL three-neck round bottom flask, then a few drops of acetic acid was added. The resulting solution was sonicated for half an hour to obtain a homogenous mixture. The flask was heated at 80 °C with stirring under argon for 48 h and cooled to room temperature. The resulting brown precipitate was collected by filtration and washed with ethanol, then vacuum dried at 60 °C for 24 h to give a red-brown powder (**TAA**) with ~80% yield.

Then A mixture of TAA (36.0 mg, 0.08 mmol) and anhydrous cobalt chloride (72.0 mg, 0.55 mmol) in DMF (2 mL) were placed in a Teflon-sealed bomb and then heated to 155 °C slowly and keep for 10 h and allowed to cool to room temperature slowly. Dark violet needle-shaped complex of **Co-TAA** was obtained, Yield (15%).

Supplementary Figures and Tables

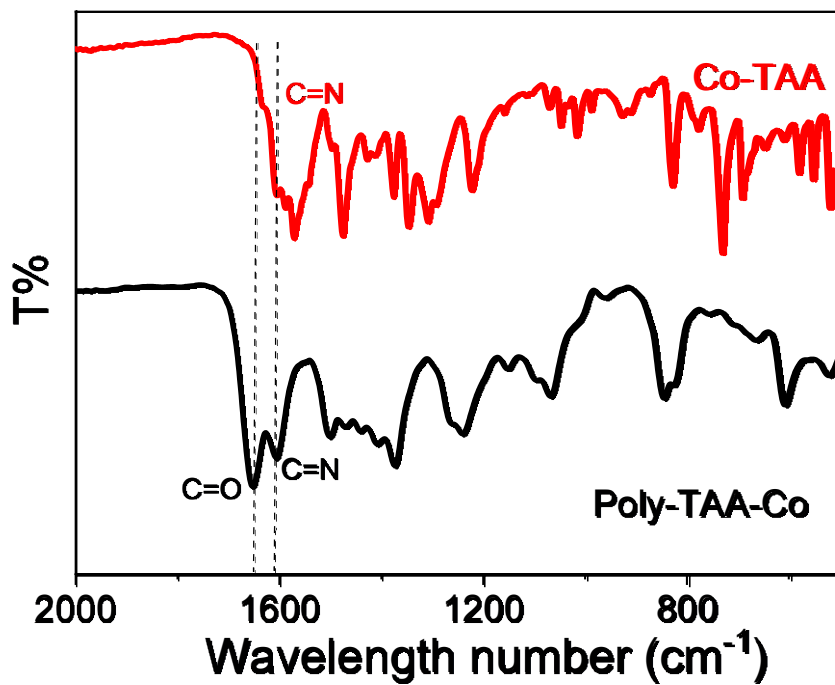


Figure S1. FT-IR spectra of the model compound Co-TAA, and Poly-TAA-Co powder.

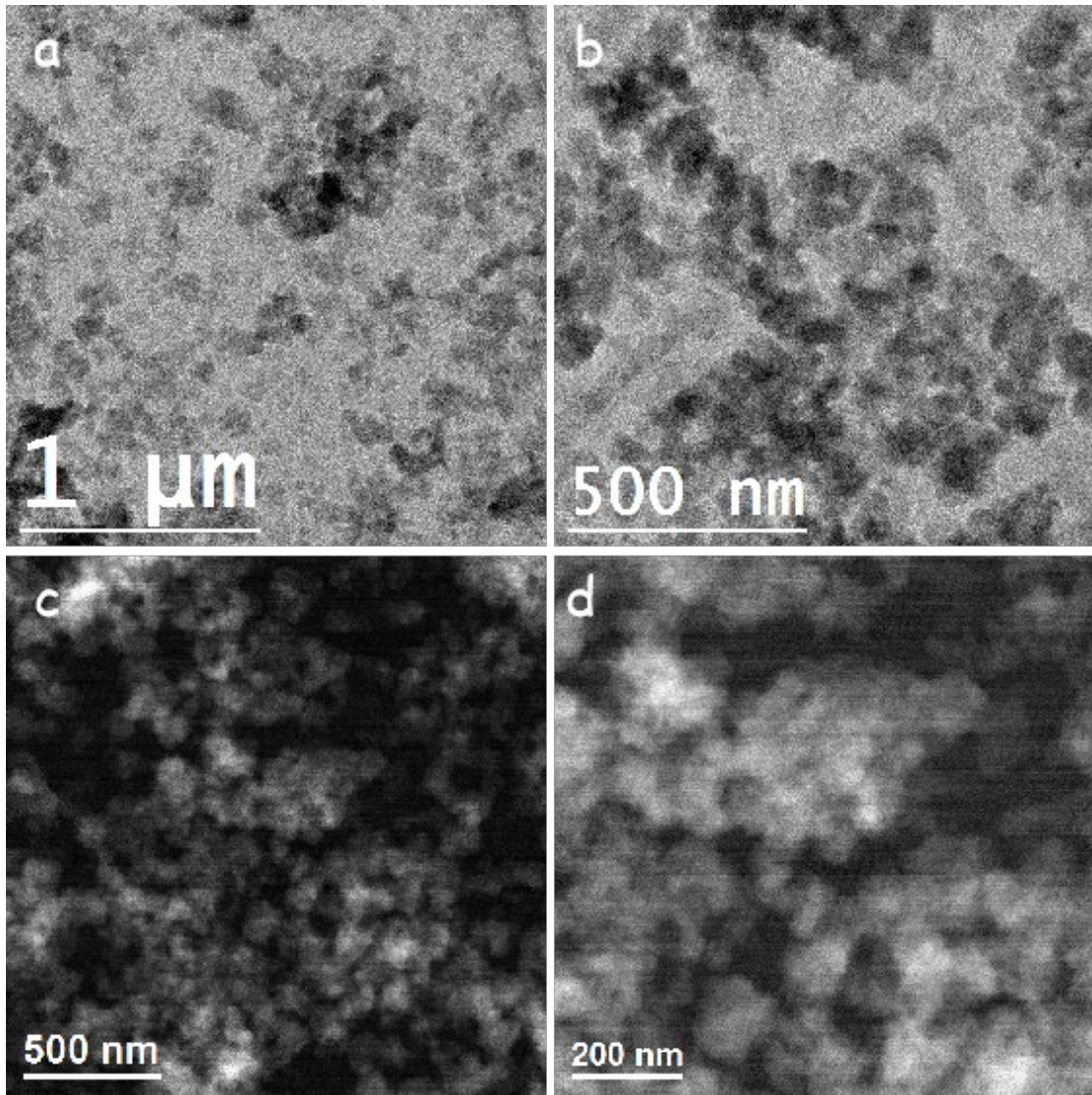


Figure S2. (a-b) HRTEM images and (c-d) STEM images of Poly-TAA-Co.

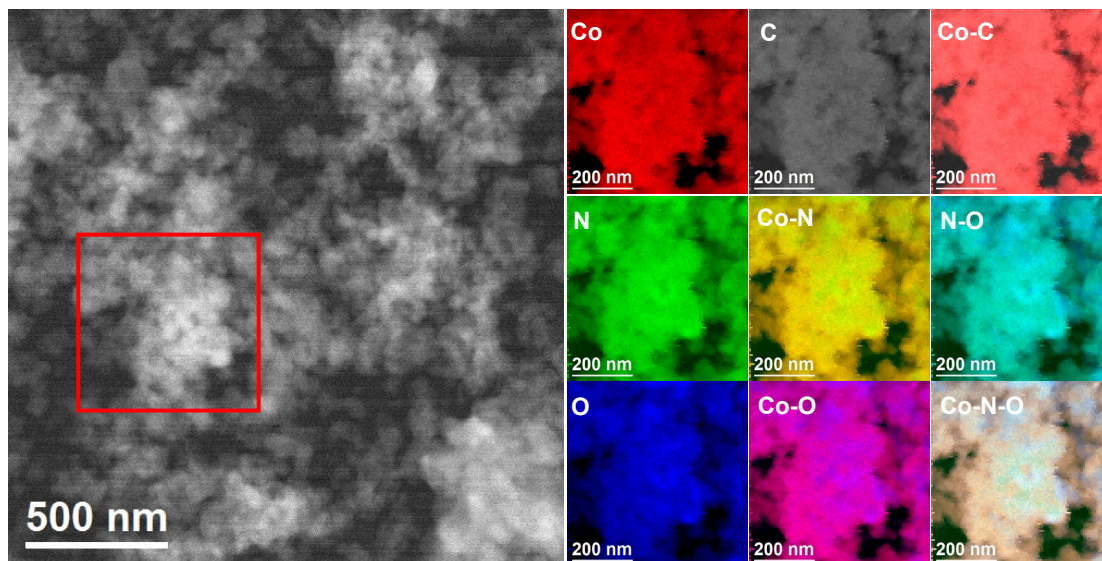


Figure S3. EELS chemical composition maps from the red squared area of the STEM micrograph. Individual Co $L_{2,3}$ -edges at 779 eV (red), N K-edges at 401 eV (green), O K-edges at 532 eV (blue), and C-K edges at 284 eV (grey) and composites of Co-N, Co-O, Co-C, N-O and Co-N-C.

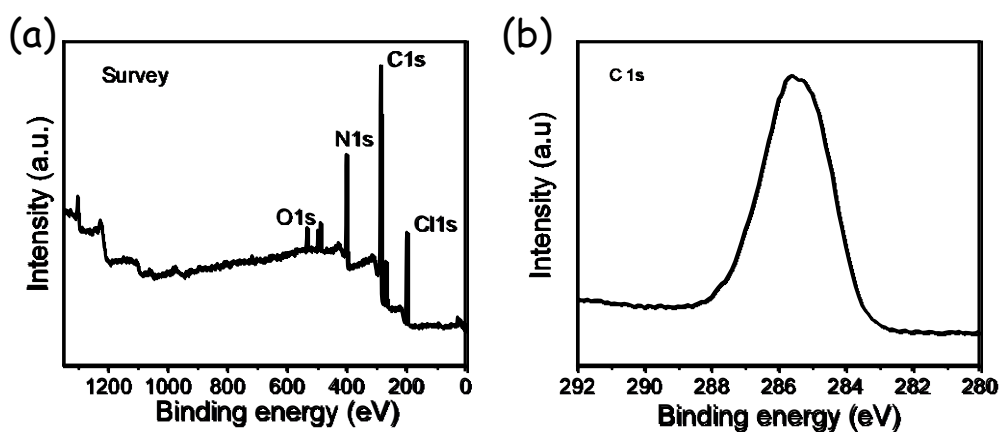


Figure S4. (a)-(b) Survey, high resolution C1s XPS spectra of Poly-TAA powder, respectively.

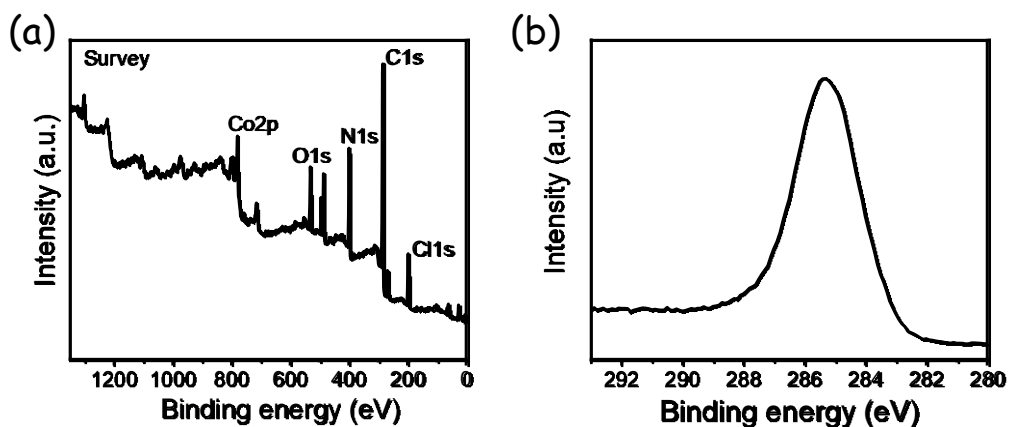


Figure S5. (a) Survey, high resolution C1s XPS spectra of Poly-TAA-Co powder, respectively.

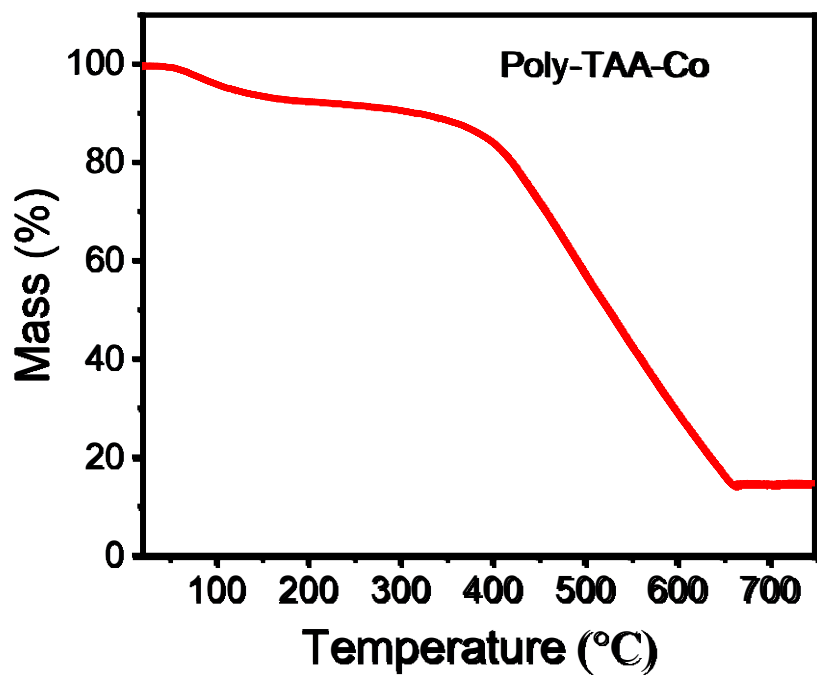


Figure S6 TGA analysis of Poly-TAA-Co under argon by heating to 600 °C at the rate of 5 °C/min.

Table S1. Co K-edge EXAFS fitting parameters for Poly-TAA-Co

Sample	Bond	R(Å)	CN	R factor (%)
Poly-TAA-Co	Co-N	2.05	3.54±0.5	0.6

R : bond length, CN: coordination number

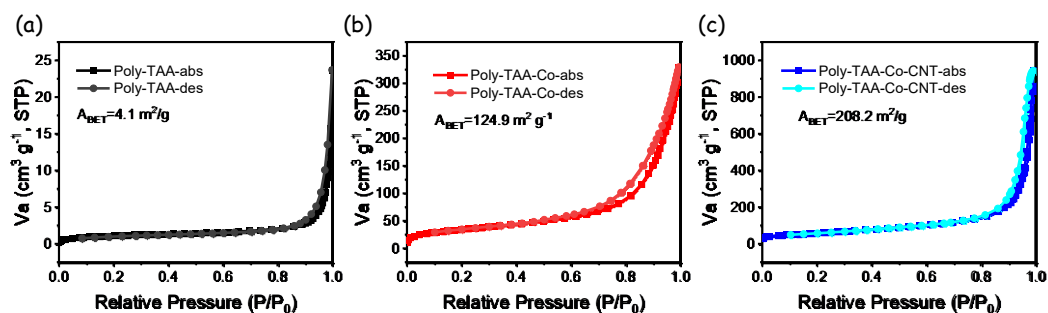


Figure S7. N₂ adsorption and desorption of Poly-TAA (a), Poly-TAA-Co (b) and Poly-TAA-Co-CNT (c), respectively.

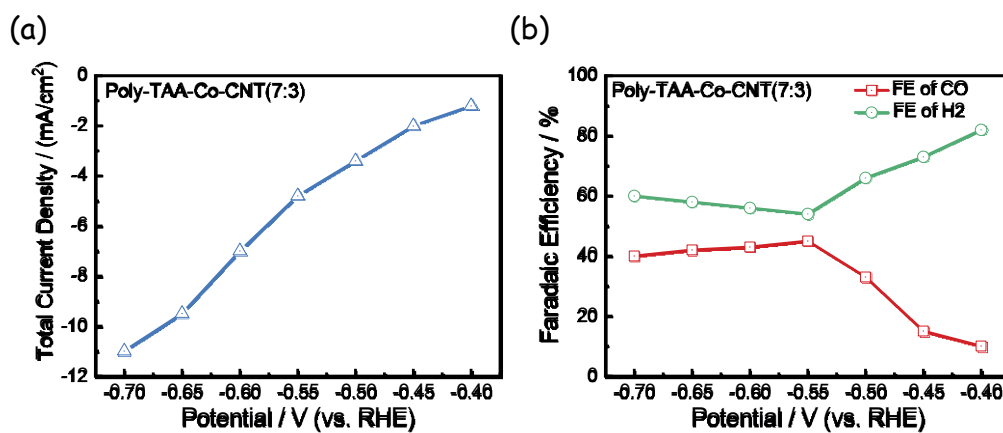


Figure S8. (a) Total current density of Poly-TAA-Co-CNT (7:3). (b) FE of CO and H₂ at various potentials for Poly-TAA-Co-CNT (7:3).

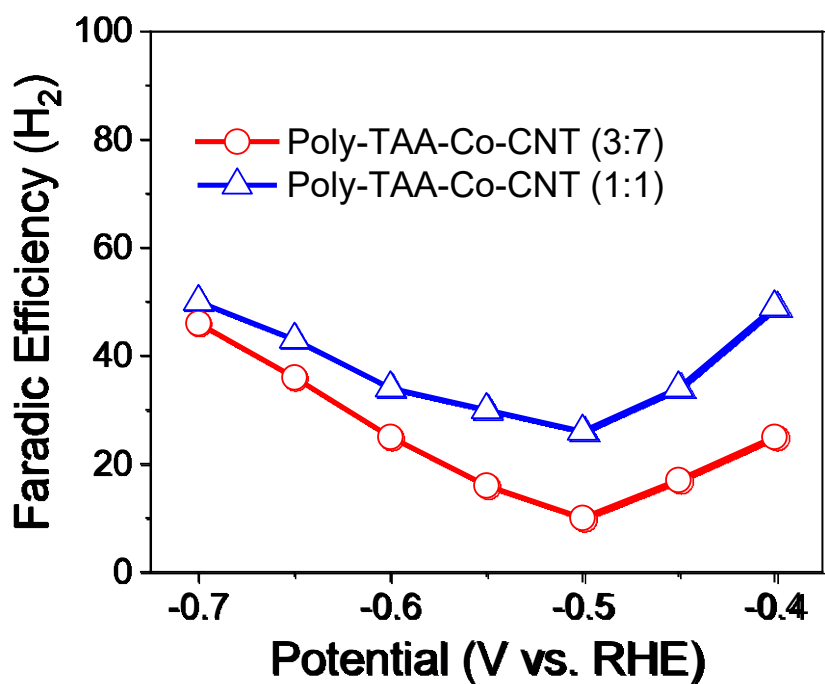


Figure S9 Current density for H₂ production on Poly-TAA-Co-CNT(1:1) and Poly-TAA-Co-CNT(3:7). and

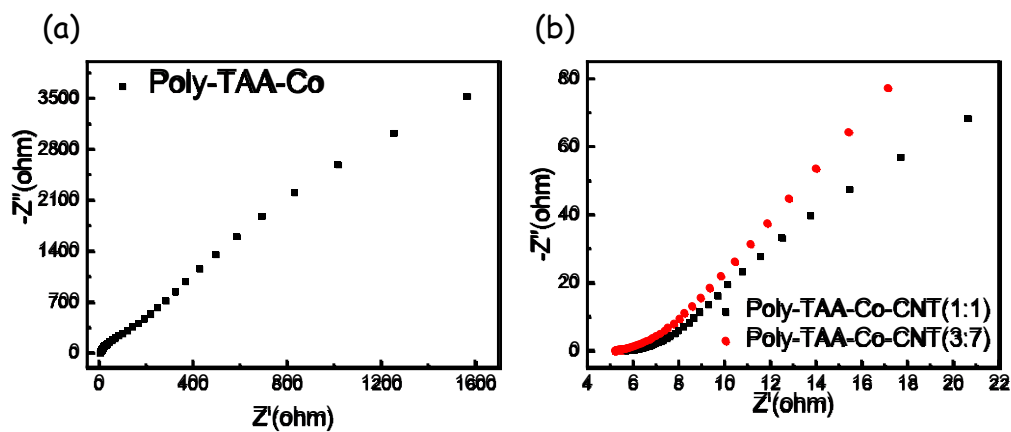


Figure S10. Nyquist plots of the electrochemical impedance spectroscopy (EIS) data of (a) Poly-TAA-Co, (b) Poly-TAA-Co-CNT(1:1) and Poly-TAA-Co-CNT(3:7) electrodes after the activation process.

The electrochemical double-layer capacitance (Cdl) curves were calculated by cyclic voltammetry (CV) in a non-Faradaic region at scan rates in the range 25 to 150 mV s⁻¹ and using the following equation: [S2]

$$C_{dl} = \Delta j / v$$

where Δj ($\Delta j = j_a - j_c$) is the current density (mA cm⁻²), and v is scan rate (mV s⁻¹), respectively. The electrochemical active surface area (ECSA) is linear with the Cdl:

$$ECSA \propto C_{dl}$$

And The surface roughness factor (Rf) is linear with the ECSA,

$$R_f \propto ECSA$$

So Rf is linear with Cdl. $R_f \propto C_{dl}$

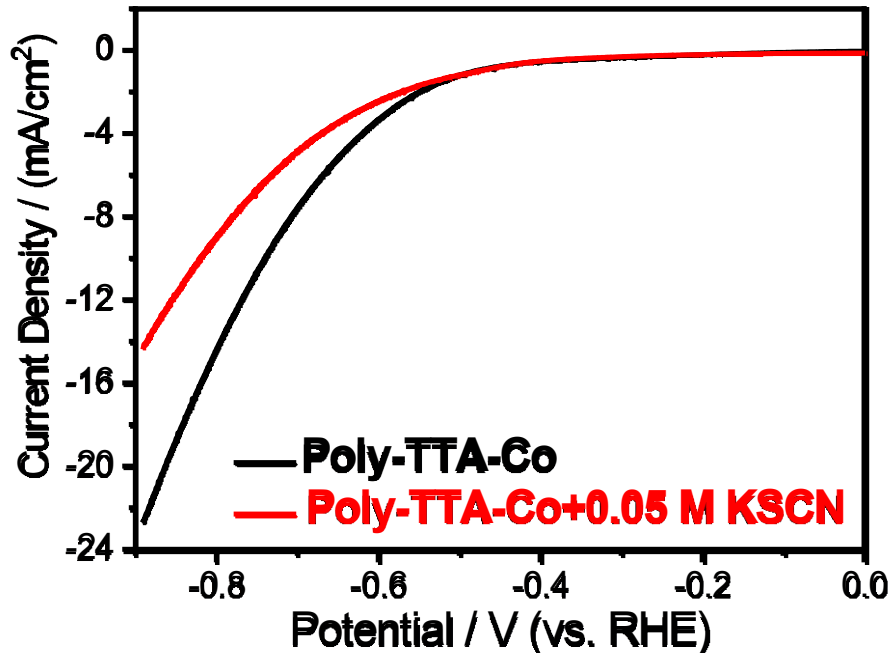


Figure S11. Linear sweep voltammetry (LSV) curves of (a) Poly-TAA-Co.

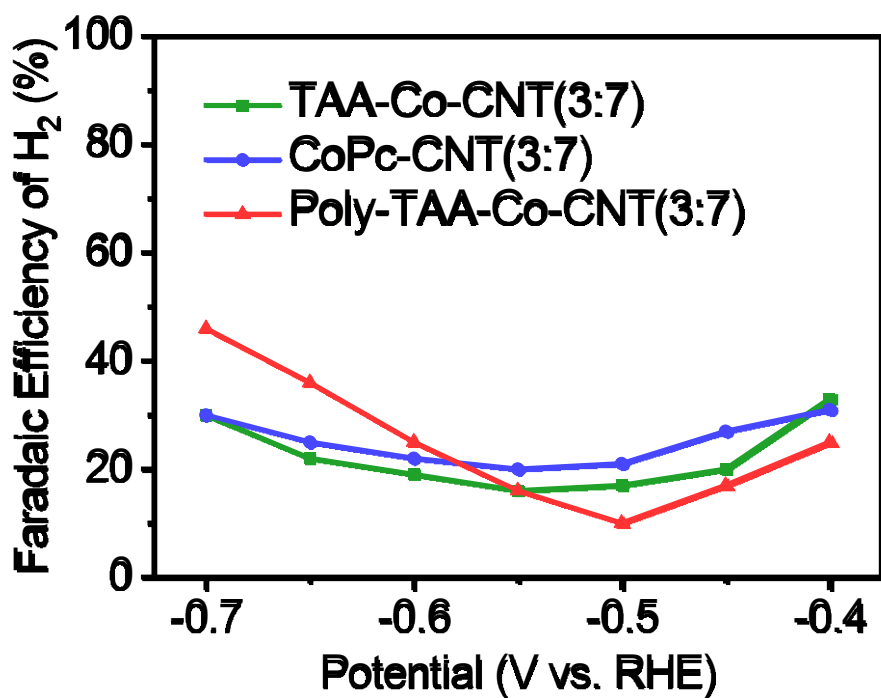


Figure S12. FE of H₂ at various potentials on Co-TAA-CNT(3:7), CoPc-CNT(3:7) and Poly-TAA-Co-CNT(3:7).

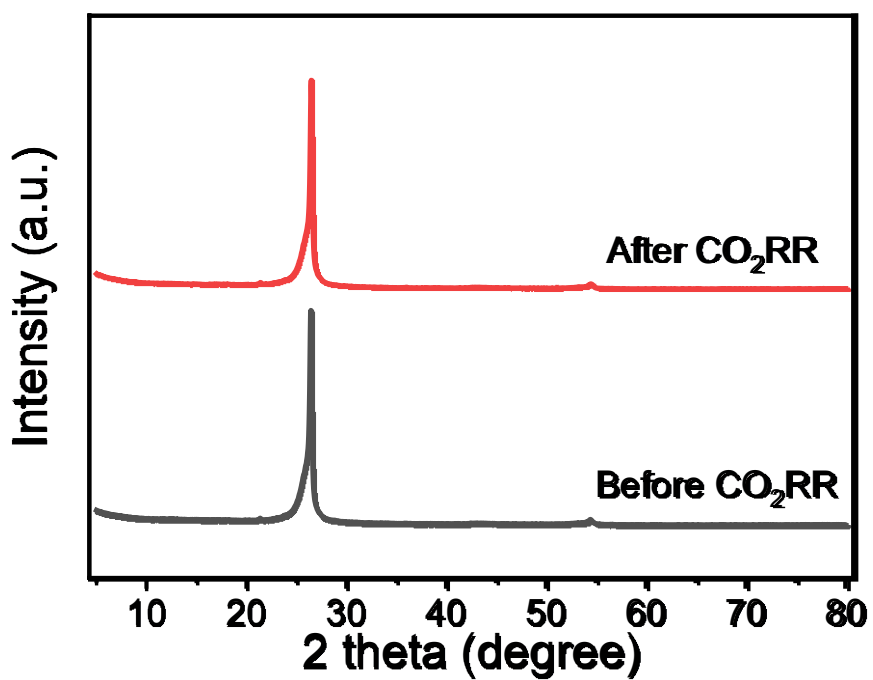


Figure S13. XRD patterns of Poly-TAA-Co-CNT loaded on carbon paper before and after CO₂RR.

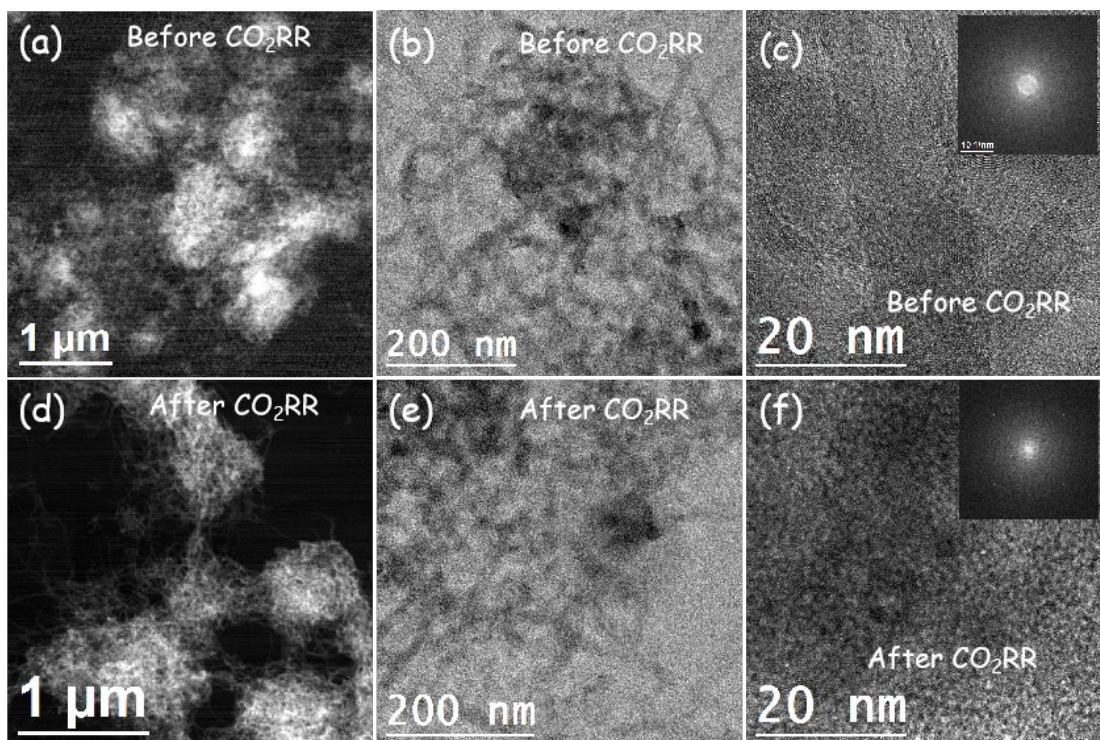


Figure S14 HAADF-STEM (a, c), BF-TEM (b, d) and HRTEM micrographs (c, e) of Poly-TAA-Co-CNT (3:7) sample (before and after CO_2RR).

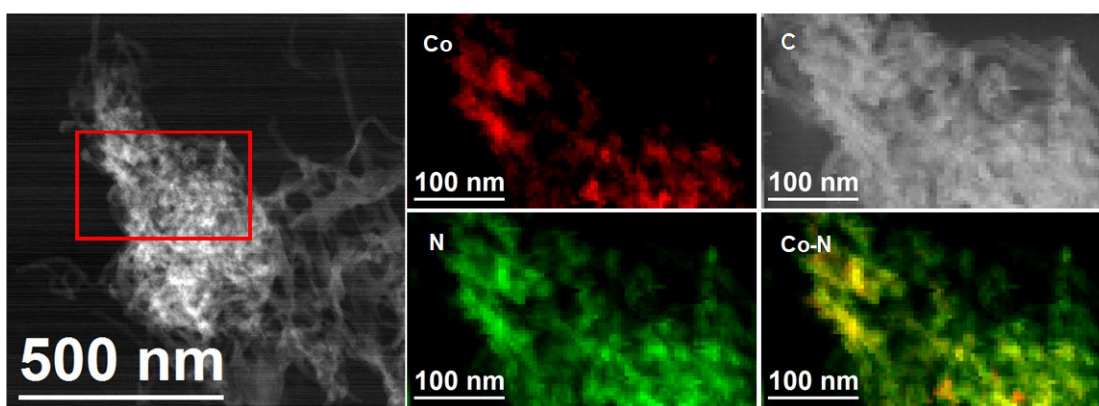


Figure S15. EELS chemical composition maps obtained from the red squared area of the STEM micrograph. Individual Co L_{2,3}-edges at 779 eV (red), N K-edges at 401 eV (green), O K-edges at 532 eV (blue), and C-K edges at 284 eV (grey) and composites of Co-N, Co-O, Co-C, N-O and Co-N-C. (Poly-TAA-Co-CNT (3:7), after electrocatalytic CO_2RR)

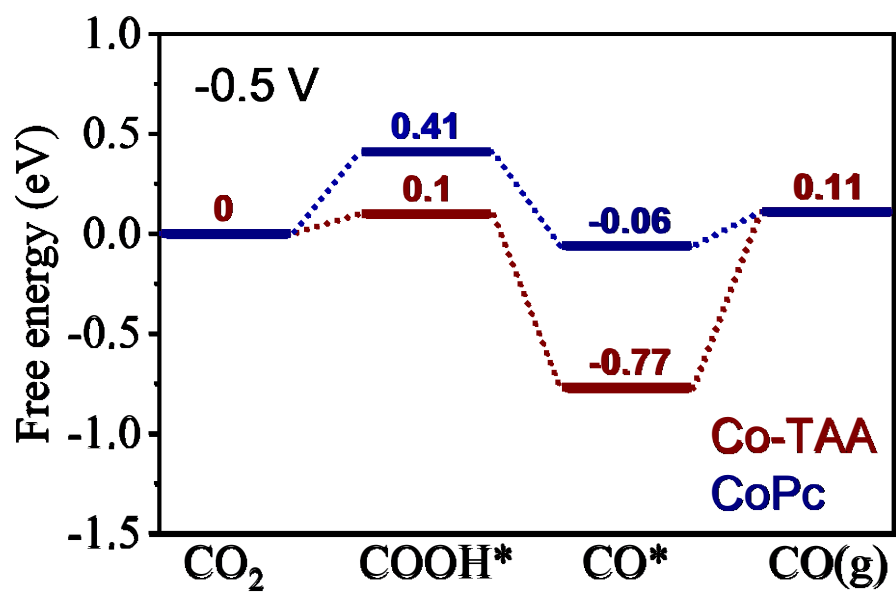


Figure S16. Calculated energy diagrams for CO₂ to CO at -0.5 V conversion on CoPc and CoTAA molecule, respectively.

Table S2. The comparison of electrochemical reduction of CO₂ to CO for reported cobalt based electrocatalysts.

Catalysts	Electrolyte	Potential (V vs RHE)	Main Product	FE _{CO} (%)	Ref.
Poly-TAA-Co-CNT	0.5 M KHCO₃	-0.5	CO	90	This work
CoPc-PI-COF-1	0.5 M KHCO ₃	-0.7	CO	93	S3
CoPc-PI-COF-1	0.5 M KHCO ₃	-0.9	CO	95	S3
CoPc-PI-COF-2	0.5 M KHCO ₃	-0.7	CO	95	S3
CoPc-PI-COF-2	0.5 M KHCO ₃	-0.9	CO	92	S3
Co-TTCOF NSs	0.5 M KHCO ₃	-0.8	CO	99.7	S18
Co-TTCOF	0.5 M KHCO ₃	-0.7	CO	91.3	S4
COF-366-Co	0.5 M KHCO ₃	-0.55	CO	90	S5
COF-366-F-Co	0.5 M KHCO ₃	-0.55	CO	87	S6
Co ₃ O ₄ -CDots-C ₃ N ₄	0.5 M KHCO ₃	-0.6	CO	89	S7
Co-PMOF	0.5 M KHCO ₃	-0.8	CO	98.7	S8
CoPPC/CNT	0.5 M KHCO ₃	-0.5	CO	85	S9

References

- [S1] H. Ryu, Y. Mulyana, In-H. Park, J. Kim, L. F. Lindoy, S. S. Lee, Discrete and polymeric complexes of a macrocyclic pillar ligand in the absence and presence of dicarboxylic acid coligands, *CrystEngComm* 17 (2015), 5717-5724.
- [S2] Z.-Q. Liu, H. Cheng, N. Li, T. Y. Ma, Y.-Z. Su, ZnCo₂O₄ Quantum Dots Anchored on Nitrogen-Doped Carbon Nanotubes as Reversible Oxygen Reduction/Evolution Electrocatalysts, *Adv. Mater.* 28 (2016), 3777-3784.
- [S3] B. Han, X. Ding, B. Yu, H. Wu, W. Zhou, W. Liu, C. Wei, B. Chen, D. Qi, H. Wang, K. Wang, Y. Chen, B. Chen, J. Jiang, Two-Dimensional Covalent Organic Frameworks with Cobalt(II)-Phthalocyanine Sites for Efficient Electrocatalytic Carbon Dioxide Reduction, *J. Am. Chem. Soc.* 143 (2021), 7104-7113.
- [S4] H. J. Zhu, M. Lu, Y. R. Wang, et al. Efficient electron transmission in covalent organic nanosheets for highly active electrocatalytic carbon dioxide reduction, *Nat. Commun.* 11 (2020), 497.
- [S5] S. Lin, C. S. Diercks, Y. B. Zhang, N. Kornienko, E. M. Nichols, Y. Zhao, A. R. Paris, D. Kim, P. Yang, O. M. Yaghi, C. J. Chang, Covalent organic frameworks comprising cobalt porphyrins for catalytic CO₂ reduction in water, *Science* 349 (2015), 1208-1213.
- [S6] C. S. Diercks, S. Lin, N. Kornienko, E. A. Kapustin, E. M. Nichols, C. Zhu, Y. Zhao, C. J. Chang, O. M. Yaghi, Reticular Electronic Tuning of Porphyrin Active Sites in Covalent Organic Frameworks for Electrocatalytic Carbon Dioxide Reduction, *J. Am. Chem. Soc.* 140 (2018), 1116-1122.
- [S7] S. Guo, et al. A Co₃O₄-CDots-C₃N₄ three component electrocatalyst design concept for efficient and tunable CO₂ reduction to syngas, *Nat. Commun.* 8 (2017), 1828.
- [S8] Y.-R. Wang, Q. Huang, C.-T. He, Y. Chen, J. Liu, F.-C. Shen, Y.-Q. Lan, Oriented electron transmission in polyoxometalate-metalloporphyrin organic framework for highly selective electroreduction of CO₂, *Nat. Commun.* 9 (2018), 4466.

[S9] N. Han, Y. Wang, L. Ma, J. Wen, J. Li, H. Zheng, K. Nie, X. Wang, F. Zhao, Y. Li, J. Fan, J. Zhong, T. Wu, D. J. Miller, J. Lu, S-T. Lee, Y. Li, Supported Cobalt Polyphthalocyanine for High-Performance Electrocatalytic CO₂ Reduction, *Chem* 3 (2017), 652-664.